

Biological network comparison using graphlet degree distribution

Nataša Pržulj

Computer Science Department, University of California, Irvine, CA 92697-3425, USA

ABSTRACT

Motivation: Analogous to biological sequence comparison, comparing cellular networks is an important problem that could provide insight into biological understanding and therapeutics. For technical reasons, comparing large networks is computationally infeasible, and thus heuristics, such as the degree distribution, clustering coefficient, diameter, and relative graphlet frequency distribution have been sought. It is easy to demonstrate that two networks are different by simply showing a short list of properties in which they differ. It is much harder to show that two networks are similar, as it requires demonstrating their similarity in *all* of their exponentially many properties. Clearly, it is computationally prohibitive to analyze all network properties, but the larger the number of constraints we impose in determining network similarity, the more likely it is that the networks will truly be similar.

Results: We introduce a new systematic measure of a network's local structure that imposes a large number of similarity constraints on networks being compared. In particular, we generalize the degree distribution, which measures the number of nodes 'touching' k edges, into distributions measuring the number of nodes 'touching' k graphlets, where graphlets are small connected non-isomorphic subgraphs of a large network. Our new measure of network local structure consists of 73 graphlet degree distributions of graphlets with 2–5 nodes, but it is easily extendible to a greater number of constraints (i.e. graphlets), if necessary, and the extensions are limited only by the available CPU. Furthermore, we show a way to combine the 73 graphlet degree distributions into a network 'agreement' measure which is a number between 0 and 1, where 1 means that networks have identical distributions and 0 means that they are far apart. Based on this new network agreement measure, we show that almost all of the 14 eukaryotic PPI networks, including human, resulting from various high-throughput experimental techniques, as well as from curated databases, are better modeled by geometric random graphs than by Erdős–Rényi, random scale-free, or Barabási–Albert scale-free networks.

Availability: Software executables are available upon request.

Contact: natasha@ics.uci.edu

1 INTRODUCTION

Understanding cellular networks is a major problem in current computational biology. These networks are commonly modeled by *graphs* (also called *networks*) with *nodes* representing biomolecules such as genes, proteins, metabolites, etc., and *edges* representing physical, chemical, or functional interactions between the biomolecules. The ability to compare such networks would be very useful. For example, comparing a diseased cellular network to a healthy one may aid in finding a cure for the disease, and comparing cellular networks of different species could enable evolutionary insights. A full description of the differences between two large networks is infeasible because it requires solving the *subgraph isomorphism* problem, which is an NP-complete problem.

Therefore, analogous to the BLAST heuristic (Altschul *et al.*, 1990) for biological sequence comparison, we need to design a heuristic tool for the full-scale comparison of large cellular networks (Berg and Lassig, 2004). The current network comparisons consist of heuristics falling into two major classes: (1) global heuristics, such as counting the number of connections between various parts of the network (the 'degree distribution'), computing the average density of node neighborhoods (the 'clustering coefficients'), or the average length of shortest paths between all pairs of nodes (the 'diameter'); and (2) local heuristics that measure relative distance between concentrations of small subgraphs (called *graphlets*) in two networks (Pržulj *et al.*, 2004).

Since cellular networks are incompletely explored, global statistics on such incomplete data may be substantially biased, or even misleading with respect to the (currently unknown) full network. Conversely, certain neighborhoods of these networks are well-studied, and so locally based statistics applied to the well-studied areas are more appropriate. A good analogy would be to imagine that MapQuest knew details of the streets of New York City and Los Angeles, but had little knowledge of highways spanning the country. Then, it could provide good driving directions inside New York or Los Angeles, but not between the two. Similarly, we have detailed knowledge of certain local areas of biological networks, but data outside these well-studied areas are currently incomplete, and so global statistics are likely to provide misleading information about the biological network as a whole, whereas local statistics are likely to be more valid and meaningful.

Owing to the noise and incompleteness of cellular network data, local approaches to analyzing and comparing cellular network structure that involve searches for small subgraphs have been successful in analyzing, modeling, and discovering functional modules in cellular networks (Milo *et al.*, 2002, 2004; Shen-Orr *et al.*, 2002; Pržulj *et al.*, 2004). Note that it is easy to show that two networks are different simply by finding any property in which they differ. However, it is much difficult to show that they are similar, since it involves showing that two networks are similar with respect to *all* of their properties. Current common approaches to show network similarity are based on listing several common properties, such as the degree distribution, clustering, diameter, or relative graphlet frequency distribution. The larger the number of common properties, the more likely it is that the two networks are similar. But any short list of properties can easily be mimicked by two very large and different networks. For example, it is easy to construct networks with exactly the same degree distribution whose structure and function differ substantially (Pržulj *et al.*, 2004; Li *et al.*, 2005; Doyle *et al.*, 2005).

In this article, we design a new local heuristic for measuring network structure that is a *direct* generalization of the degree distribution. In fact, the degree distribution is the first in the spectrum of 73 graphlet degree distributions that are components of this

new measure of network structure. Thus, in our new network similarity measure, we impose 73 highly structured constraints in which networks must show similarity to be considered similar; this is a much larger number of constraints than provided by any of the previous approaches and, therefore, it increases the chances that two networks are truly similar if they are similar with respect to this new measure. Moreover, the measure can be easily extended to a greater number of constraints simply by adding more graphlets. The extensions are limited only by the available CPU.

Based on this new measure of structural similarity between two networks, we show that the geometric random graph model shows exceptionally high agreement with 12 out of 14 different eukaryotic protein–protein interaction (PPI) networks. Furthermore, we show that such high structural agreements between PPI and geometric random graphs are unlikely to be beaten by another random graph model, at least under this measure.

1.1 Background

Large amounts of cellular network data for a number of organisms have recently become available through high-throughput methods (Ito *et al.*, 2000; Uetz *et al.*, 2000; Giot *et al.*, 2003; Li *et al.*, 2004; Stelzl *et al.*, 2005; Rual *et al.*, 2005). Statistical and theoretical properties of these networks have been extensively studied (Jeong *et al.*, 2000; Maslov and Sneppen, 2002; Shen-Orr *et al.*, 2002; Milo *et al.*, 2002; Vazquez *et al.*, 2004; Yeager-Lotem *et al.*, 2004; Pržulj *et al.*, 2004; Tanaka, 2005) owing to their important biological implications (Jeong *et al.*, 2001; Lappe and Holm, 2004).

Comparing large cellular networks is computationally intensive. Exhaustively computing the differences between networks is computationally infeasible, and thus efficient heuristic algorithms have been sought (Kashtan *et al.*, 2004; Pržulj *et al.*, 2006). Although *global properties* of large networks are easy to compute, they are inappropriate for use on incomplete networks because they can at best describe the structure produced by the biological sampling techniques used to obtain the partial networks (Han *et al.*, 2005). Therefore, bottom-up or *local* heuristic approaches for studying network structure have been proposed (Milo *et al.*, 2002; Shen-Orr *et al.*, 2002; Pržulj *et al.*, 2004). Analogous to sequence motifs, *network motifs* have been defined as subgraphs that occur in a network at frequencies much higher than expected at random (Milo *et al.*, 2002; Shen-Orr *et al.*, 2002; Milo *et al.*, 2004). Network motifs have been generalized to *topological motifs* as recurrent ‘similar’ network sub-patterns (Berg and Lassig, 2004). However, the approaches based on network motifs ignore infrequent subnetworks and subnetworks with ‘average’ frequencies, and thus are not sufficient for full-scale network comparison. Therefore, small connected non-isomorphic induced subgraphs of a large network, called *graphlets*, have been introduced to design a new measure of local structural similarity between two networks based on their relative frequency distributions (Pržulj *et al.*, 2004).

The earliest attempts to model real-world networks include *Erdős–Rényi random graphs* (henceforth denoted by ‘ER’) in which edges between pairs of nodes are distributed uniformly at random with the same probability p (Erdős and Rényi, 1959, 1960). This model poorly describes several properties of real-world networks, including the degree distribution and clustering coefficients, and therefore it has been refined into *generalized random graphs* in which the edges are randomly chosen as in ER random graphs, but the degree distribution is constrained to match the degree

distribution of the real network (henceforth, we denote these networks by ‘ER-DD’). Matching other global properties of the real-world networks to the model networks, such as clustering coefficients, lead to further improvements in modeling real-world networks including *small-world* (Watts and Strogatz, 1998; Newman and Watts, 1999a, b) and *scale-free* (Simon, 1955; Barabási and Albert, 1999) network models (henceforth, we denote by ‘SF’ scale-free Barabási–Albert networks). Many cellular networks have been described as scale-free (Barabási and Oltvai, 2004). However, this issue has been heavily debated (de Aguiar and Bar-Yam, 2005; Stumpf *et al.*, 2005; Han *et al.*, 2005; Tanaka, 2005). Recently, based on the local relative graphlet frequency distribution measure, a geometric random graph model (Penrose, 2003) has been proposed for high-confidence PPI networks (Pržulj *et al.*, 2004).

2 APPROACH

In Section 2.1, we describe the 14 PPI networks and the four network models that we analyzed. Then we describe how we generalize the degree distribution to our spectrum of graphlet degree distributions (Section 2.2); note that the degree distribution is the first distribution in this spectrum, since it corresponds to the only graphlet with two nodes. Finally, we construct a new measure of similarity between two networks based on graphlet degree distributions (Section 2.3). We describe the results of applying this measure to the 14 PPI networks in Section 3.

2.1 PPI and model networks

We analyzed PPI networks of the eukaryotic organisms yeast *Saccharomyces cerevisiae*, fruitfly *Drosophila melanogaster*, nematode worm *Caenorhabditis elegans*, and human. Several different datasets are available for yeast and human, so we analyzed five yeast PPI networks obtained from three different high-throughput studies (Uetz *et al.*, 2000; Ito *et al.*, 2000; von Mering *et al.*, 2002) and five human PPI networks obtained from the two recent high-throughput studies (Stelzl *et al.*, 2005; Rual *et al.*, 2005) and three curated databases (Bader *et al.*, 2003; Peri *et al.*, 2004; Zanzoni *et al.*, 2002). We denote by ‘YHC’ the high-confidence yeast PPI network as described by von Mering *et al.* (2002), by ‘Y11K’ the yeast PPI network defined by the top 11 000 interactions in the von Mering *et al.* (2002) classification, by ‘YIC’ the Ito *et al.* (2000) ‘core’ yeast PPI network, by ‘YU’ the Uetz *et al.* (2000) yeast PPI network, and by ‘YICU’ the union of Ito *et al.* (2000) core and Uetz *et al.* (2000) yeast PPI networks [we unioned them as did Han *et al.* (2005) to increase coverage]. ‘FE’ and ‘FH’ denote the fruitfly *D.melanogaster* entire and high-confidence PPI networks published by Giot *et al.* (2003). Similarly, ‘WE’ and ‘WC’ denote the worm *C.elegans* entire and ‘core’ PPI networks published by Li *et al.* (2005). Finally, ‘HS’, ‘HG’, ‘HB’, ‘HH’, and ‘HM’ stand for human PPI networks by Stelzl *et al.* (2005), Rual *et al.* (2005), from BIND (Bader *et al.*, 2003), HPRD (Peri *et al.*, 2004), and MINT (Zanzoni *et al.*, 2002), respectively [BIND, HPRD, and MINT data have been downloaded from OPHID (Brown and Jurisica, 2005) on February 10, 2006]. Note that these PPI networks come from a wide array of experimental techniques; e.g. YHC and Y11K are mainly coming from tandem affinity purifications (TAP) and high-throughput MS/MS protein complex identification (HMS-PCI), whereas YIC, YU, YICU,

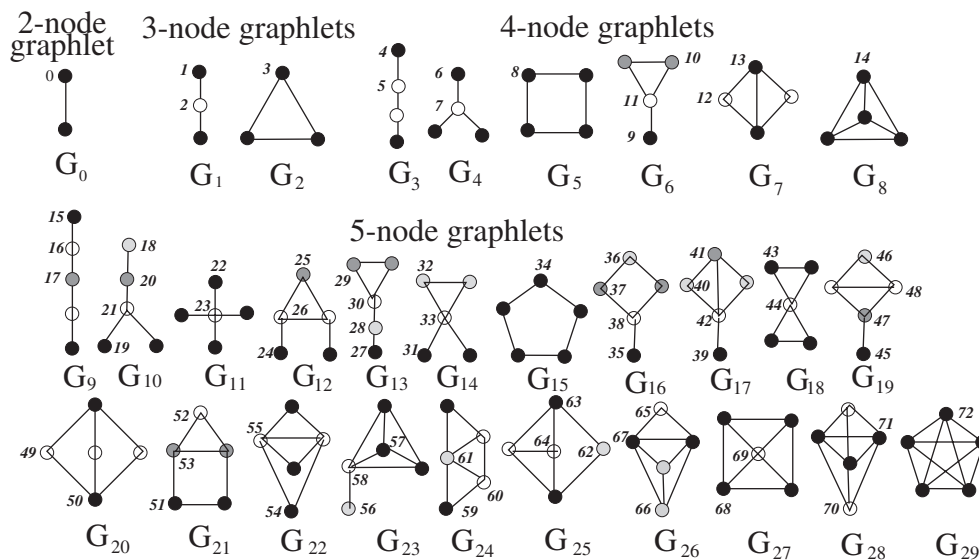


Fig. 1. Automorphism orbits $0, 1, 2, \dots, 72$ for the thirty 2, 3, 4, and 5-node graphlets G_0, G_1, \dots, G_{29} . In a graphlet G_i , $i \in \{0, 1, \dots, 29\}$, nodes belonging to the same orbit are of the same shade.

FE, FH, WE, WH, HS, and HG are yeast two-hybrid (Y2H), and HB, HH, and HM are a result of human curation (BIND, HPRD, and MINT).

The four network models that we compared against the above 14 PPI networks are ER, ER-DD, SF, and 3-dimensional geometric random graphs (henceforth denoted by ‘GEO-3D’). Model networks corresponding to a PPI network have the same number of nodes and the number of edges within 1% of the PPI network’s [details of the construction of model networks are presented by Pržulj *et al.* (2006)]. For each of the 14 PPI networks, we constructed and analyzed 25 networks belonging to each of these 4 network models. Thus, we analyzed the total of $14 + (14 \times 4 \times 25) = 1414$ networks. We compared the agreement of each of the 14 PPI networks with each of the corresponding $4 \times 25 = 100$ model networks described above (our new agreement measure is described in Section 2.3). The results of this analysis are presented in Section 3.

2.2 Graphlet degree distribution (GDD)

We generalize the notion of the degree distribution as follows. The degree distribution measures, for each value of k , the number of nodes of degree k . In other words, for each value of k , it gives the number of nodes ‘touching’ k edges. Note that an edge is the only graphlet with two nodes; henceforth, we call this graphlet G_0 (illustrated in Fig. 1). Thus, the degree distribution measures the following: how many nodes ‘touch’ one G_0 , how many nodes ‘touch’ two G_0 s, \dots , how many nodes ‘touch’ k G_0 s. Note that there is nothing special about graphlet G_0 and that there is no reason not to apply the same measurement to other graphlets. Thus, in addition to applying this measurement to an edge, i.e. graphlet G_0 , as in the degree distribution, we apply it to the 29 graphlets G_1, G_2, \dots, G_{29} presented in Figure 1 as well.

When we apply this measurement to graphlets G_0, G_1, \dots, G_{29} , we need to take care of certain topological issues that we first illustrate in the following example and then define formally. For graphlet G_1 , we ask how many nodes touch a G_1 ; however, note

that it is topologically relevant to distinguish between nodes touching a G_1 at an end or at the middle node. This is due to the following mathematical property of G_1 : a G_1 admits an automorphism (defined below) that maps its end nodes to each other and the middle node to itself. To understand this phenomenon, we need to recall the following standard mathematical definitions. An *isomorphism* g from graph X to graph Y is a bijection of nodes of X to nodes of Y such that xy is an edge of X if and only if $g(x)g(y)$ is an edge of Y ; an *automorphism* is an isomorphism from a graph to itself. The automorphisms of a graph X form a *group*, called the *automorphism group* of X , and is commonly denoted by $\text{Aut}(X)$. If x is a node of graph X , then the *automorphism orbit* of x is $\text{Orb}(x) = \{y \in V(X) \mid y = g(x) \text{ for some } g \in \text{Aut}(X)\}$, where $V(X)$ is the set of nodes of graph X . Thus, end nodes of a G_1 belong to one automorphism orbit, whereas the mid-node of a G_1 belongs to another. Note that graphlet G_0 (i.e. an edge) has only one automorphism orbit, as does graphlet G_2 ; graphlet G_3 has two automorphism orbits, as does graphlet G_4 , graphlet G_5 has one automorphism orbit, graphlet G_6 has three automorphism orbits, etc. (Fig. 1). In Figure 1, we illustrate the partition of nodes of graphlets G_0, G_1, \dots, G_{29} into automorphism orbits (or just *orbits* for brevity); henceforth, we number the 73 different orbits of graphlets G_0, G_1, \dots, G_{29} from 0 to 72, as illustrated in Figure 1. Analogous to the *degree distribution*, for each of these 73 automorphism orbits, we count the number of nodes touching a particular graphlet at a node belonging to a particular orbit. For example, we count how many nodes touch one triangle (i.e. graphlet G_2), how many nodes touch two triangles, how many nodes touch three triangles, etc. We need to separate nodes touching a G_1 at an end-node from those touching it at a mid-node; thus, we count how many nodes touch one G_1 at an end-node (i.e. at orbit 1), how many nodes touch two G_1 s at an end-node, how many nodes touch three G_1 s at an end-node, etc. and also how many nodes touch one G_1 at a mid-node (i.e. at orbit 2), how many nodes touch two G_1 s at a mid-node, how many nodes touch three G_1 s at a mid-node, etc. In this way, we obtain 73 distributions analogous to the degree distribution

(actually, the degree distribution is the distribution for the 0-th orbit, i.e. for graphlet G_0). Thus, the degree distribution, which has been considered to be a global network property, is one in the *spectrum* of 73 ‘graphlet degree distributions (GDDs)’ measuring local structural properties of a network. Note that GDD is measuring *local* structure, since it is based on small local network neighborhoods. The distributions are unlikely to be statistically independent of each other, although we have not yet worked out the details of the interdependence.

2.3 Network ‘GDD agreement’

There are many ways to ‘reduce’ the large quantity of numbers representing 73 sample distributions. In this section, we describe one way; there may be better ways, and certainly finding better ways to reduce this data is an obvious future direction. Some of the details may seem obscure at first; we justify them at the end of this section.

We start by measuring the 73 GDDs for each network that we wish to compare. Let G be a network (i.e. a graph). For a particular automorphism orbit j (refer to Fig. 1), let $d_G^j(k)$ be the sample distribution of the number of nodes in G touching the appropriate graphlet (for automorphism orbit j) k times. That is, d_G^j represents the j -th graphlet degree distribution (GDD). We scale $d_G^j(k)$ as

$$S_G^j(k) = \frac{d_G^j(k)}{k} \quad (1)$$

to decrease the contribution of larger degrees in a GDD (for reasons we describe later that are illustrated in Fig. 2), and then normalize the distribution with respect to its total area¹,

$$T_G^j = \sum_{k=1}^{\infty} S_G^j(k). \quad (2)$$

giving the ‘normalized distribution’

$$N_G^j(k) = \frac{S_G^j(k)}{T_G^j}. \quad (3)$$

In words, $N_G^j(k)$ is the fraction of the total area under the curve, over the entire GDD, devoted to degree k . Finally, for two networks G and H and a particular orbit j , we define the ‘distance’ $D^j(G, H)$ between their normalized j -th distributions as

$$D^j(G, H) = \left(\sum_{k=1}^{\infty} [N_G^j(k) - N_H^j(k)]^2 \right)^{1/2}, \quad (4)$$

where again in practice the upper limit of the sum is finite due to the finite sample. The distance is between 0 and 1, where 0 means that G and H have identical j -th GDDs, and 1 means that their j -th GDDs are far away. Next, we reverse $D^j(G, H)$ to obtain the j -th GDD agreement:

$$A^j(G, \pm H) = 1 - D^j(G, H), \quad (5)$$

for $j \in \{0, 1, \dots, 72\}$. Finally, the *agreement* between two networks G and H is either the arithmetic [Equation (6)] or geometric [Equation (7)] mean of $A^j(G, H)$ over all j , i.e.

$$A_{\text{arith}}(G, H) = \frac{1}{73} \sum_{j=0}^{72} A^j(G, H), \quad (6)$$

¹In practice the upper limit of the sum is finite owing to finite sample size.

and

$$A_{\text{geo}}(G, H) = \left(\prod_{j=0}^{72} A^j(G, H) \right)^{1/73}. \quad (7)$$

Now we give the rationale for designing the agreement measure in this way. There are many different ways to design a measure of agreement between two distributions. They are all heuristic, and thus one needs to examine the data to design the agreement measure that works best for a particular application. The justification of our choice of the graphlet degree distribution agreement measure can be illustrated by an example of two GDDs for the yeast high-confidence PPI network (von Mering *et al.*, 2002) and the corresponding 3-dimensional geometric random networks presented in Figure 2. This figure gives an illustration of the GDDs of orbit 11 of the PPI and average GDD of orbit 11 in 25 model networks (panel A) being ‘closer’ than the GDDs of orbit 16 (panel B); this is accurately reflected by our agreement measure which gives an agreement of 0.89 for orbit 11 GDDs and of 0.51 for orbit 16. However, note that the sample distributions extend in the x -axis out to degrees of 10^4 or even 10^5 ; we believe that most of the ‘information’ in the distribution is contained in the lower degrees and that the information in the extreme high degrees is noise due to bio-technical false positives caused by auto-activators or sticky proteins (Han *et al.*, 2005). However, without scaling by $1/k$ as in Equation (1), both the area under the curve (2) and the distance (4) would be dominated by the counts for large k . This explains the scaling in Equation (1). The ‘normalization’, Equation (3), is performed in order to force both distributions to have a total area under the curve of 1 before they are compared. We can now compute, for each value of k , the ‘distance’ between two distributions at that value of k . Formally, k is unbounded but in practice it is finite due to the finite size of the graph. We then treat the vector of distances as a vector in the unit cube of dimension equal to the maximum value of k . We compute the Euclidean distance between two of these vectors, representing two networks, in Equation (4). Finally, we choose to switch from ‘distance’ to ‘agreement’ in Equation (5) simply because we feel agreement is a more intuitive measure.

To gauge the quality of this agreement measure, we computed the average agreements between various model (i.e. theoretical) networks. For example, when comparing networks of the same type (ER versus ER, ER-DD versus ER-DD, GEO-3D versus GEO-3D, or SF versus SF), we found the mean agreement to be 0.84 with a standard deviation of 0.07. To verify that our ‘agreement’ measure can give low values for networks that are very different, we also constructed a ‘straw-man’ model graph called a *circulant* (West, 2001), and compared it with some actual PPI network data. A circulant graph is constructed by adding ‘chords’ to a *cycle* on n nodes (examples of cycles on 3, 4, and 5 nodes are graphlets G_2 , G_5 , and G_{15} , respectively) so that i -th node on the cycle is connected to the $[(i+j) \bmod n]$ -th and $[(i-j) \bmod n]$ -th node on the cycle. Clearly, a large circulant with an equal number of nodes and edge density as the data would not be very representative of a PPI network, and indeed we find that the agreement between such a circulant, with chords defined by $j \in \{6, 12\}$, and the data is < 0.08 . Note that in most of the 14 PPI networks, the number of edges is about three times the number of nodes, so we chose circulants with three times as many edges as nodes; also, we

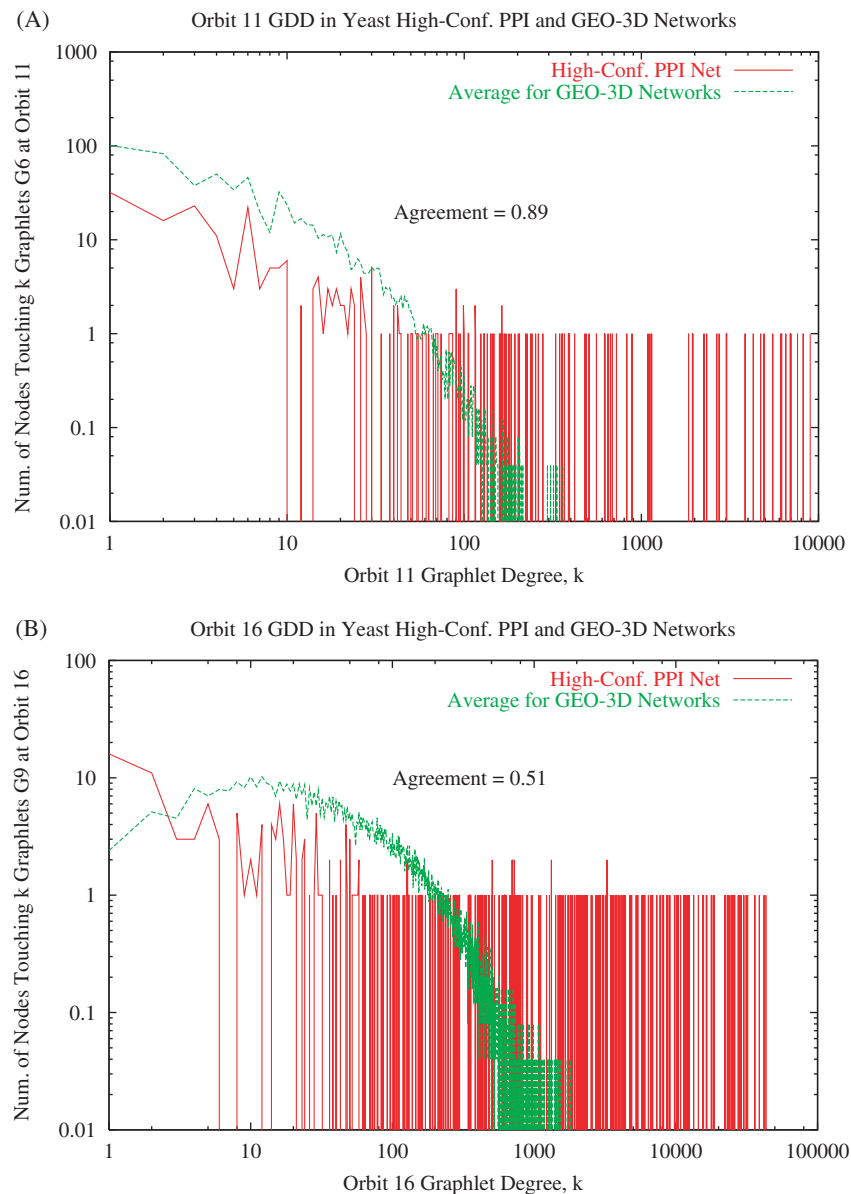


Fig. 2. Examples of graphlet degree distributions (GDDs) for yeast high-confidence PPI network (von Mering *et al.*, 2002) (solid red line) and the average of 25 corresponding 3-dimensional geometric random networks (GEO-3D, dashed green line): (A) Orbit 11; (B) Orbit 16. Most counts beyond about $k = 20$ are zero, with a few instances of 1 or (very occasionally) 2. This results in a large amount of red and green ink which is mostly noise, as the distribution fluctuates frequently from 1 to 0 (which is $-\infty$ on our log scale). The noise could be reduced by applying a broad-band filter, but we have chosen to leave the data in its raw state, despite the deleterious effect on the aesthetics of the plot.

chose $j > 5$ to maximize the number of 3, 4, and 5-node graphlets that do not occur in the circulant, since all of the 3, 4, and 5-node graphlets occur in the data.

3 RESULTS AND DISCUSSION

We present the results of applying the newly introduced ‘agreement’ measure (Section 2.3) to 14 eukaryotic PPI networks and their corresponding model networks of four different network model types (described in Section 2.1). The results show that

3-dimensional geometric random graphs have exceptionally high agreement with all of the 14 PPI networks.

We undertook a large-scale scientific computing task by implementing the above described new methods and using them to compare agreements across the 4 random graph models of 14 real PPI networks. Using these new methods, we analyzed a total of 1414 networks: 14 eukaryotic PPI networks of varying confidence levels described in Section 2.1 and 25 model networks per random graph model corresponding to each of the 14 PPI networks, where random graph models were ER, ER-DD, SF, and GEO-3D (described in Section 2.1). The largest of these networks

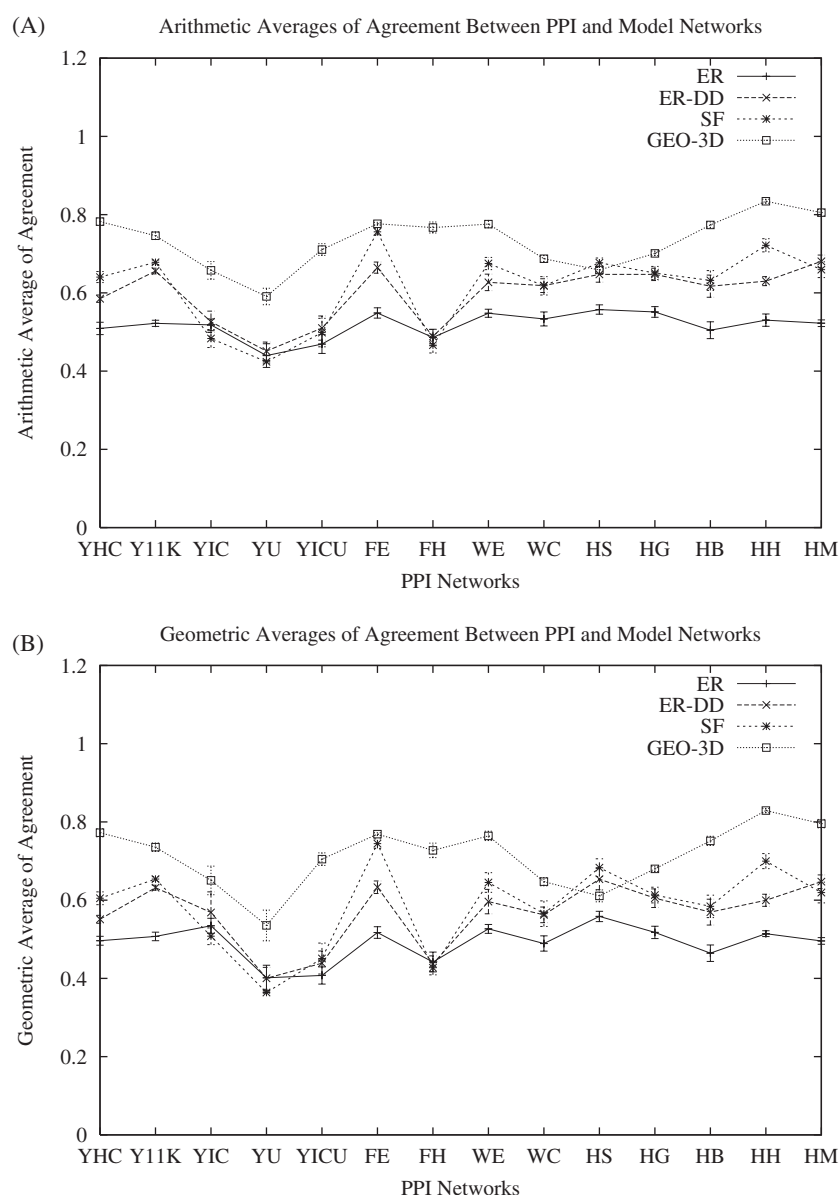


Fig. 3. Agreements between the 14 PPI networks and their corresponding model networks. Labels on the horizontal axes are described in Section 2.1. Averages of agreements between 25 model networks and the corresponding PPI network are presented for each random graph model and each PPI network, i.e. at each point in the figure; the error bar around a point is 1 SD below and above the point (in some cases, error bars are barely visible, since they are of the size of the point). As described in Section 2.3, the agreement between a PPI and a model network is based on the: (A) arithmetic average of j -th GDD agreements; and (B) geometric average of j -th GDD agreements.

had around 7000 nodes and over 20 000 edges. For each of the 14 PPI networks and each of the 4 random graph models, we computed averages and standard deviations of graphlet degree distribution (GDD) *agreements* between the PPI and the 25 corresponding model networks belonging to the same random graph model. The results are presented in Figure 3.

ER networks show ~ 0.5 agreement with each of the PPI networks whereas scale-free networks of type ER-DD and SF show a slightly improved agreement (ER-DD networks are random scale-free, since the degree distributions forced on them by the corresponding PPI networks roughly follow power law). Note that GEO-3D networks

show the highest agreement for *all* but 1 of the 14 PPI networks (Fig. 3). For HS PPI network, it is not clear which of the GEO-3D, SF, and ER-DD models agrees the most with the data, since the average agreements of HS network with these models are about the same and within 1 SD from each other. GEO-3D and SF model are similarly tied for the FE network. Since networks belonging to the same random graph model have average agreement of 0.84 with a standard deviation of 0.07 (shown in Section 2.3), the agreements of >0.7 , that most of the PPI networks have with the GEO-3D model, are very good. Note that 8 out of the 14 PPI networks have agreements with GEO-3D model of >0.75 ; since

networks of the same type agree on average by 0.84 ± 0.07 , we conclude that the agreements of 0.75 are exceptionally high and are unlikely to be beaten by another network model under this measure. Also, it is interesting that GEO-3D model shows high agreement with PPI networks obtained from various experimental techniques (Y2H, TAP, HMS-PCI) as well as from human curation (see Section 2.1). Note that this does not mean that GEO-3D is the best possible model. For example, it may be possible to construct a different ‘agreement’ measure that is more sensitive and under which a model better than GEO-3D may be apparent. However, we believe that the current ‘agreement’ measure is sensitive and meaningful enough to conclude that GEO-3D is a better model than ER, ER-DD, and SF.

4 CONCLUSION

We have constructed a new measure of structural similarity between large networks based on the graphlet degree distribution. The degree distribution is the first one in the sequence of graphlet degree distributions that are constructed in a structured and systematic way to impose a large number of constraints on the structure of networks being compared. This new measure is easily extendible to a greater number of constraints simply by adding more graphlets to those in Figure 1, although this would add significantly to the cost of computing agreements; the extensions are limited only by the available CPU. Based on this new network similarity measure, we have shown that almost all of the 14 eukaryotic PPI networks resulting from various high-throughput experimental techniques, as well as curated databases, are better modeled by geometric random graphs than by Erdős–Rényi, random scale-free, or Barabási–Albert scale-free networks. This suggests that a biological description of the (possibly *metric*) space of PPIs may help us to understand their evolution.

ACKNOWLEDGEMENTS

We thank Derek Corneil and Wayne Hayes for helpful comments and discussions, Pierre Baldi for providing computing resources and Jason Lai for help with programming.

REFERENCES

- Altschul,S.F. *et al.* (1990) Basic local alignment search tool. *J. Mol. Biol.*, **215**, 403–410.
- Bader,G.D. *et al.* (2003) BIND: the biomolecular interaction network database. *Nucleic Acids Res.*, **31**, 248–250.
- Barabási,A.L. and Albert,R. (1999) Emergence of scaling in random networks. *Science*, **286**, 509–512.
- Barabási,A.-L. and Oltvai,Z.N. (2004) Network biology: understanding the cell’s functional organization. *Nat. Rev.*, **5**, 101–113.
- Berg,J. and Lassig,M. (2004) Local graph alignment and motif search in biological networks. *Proc. Natl Acad. Sci. USA*, **101**, 14689–14694.
- Brown,K. and Jurisica,I. (2005) Online predicted human interaction database. *Bioinformatics*, **21**, 2076–2082.
- de Aguiar,M.A.M. and Bar-Yam,Y. (2005) Spectral analysis and the dynamic response of complex networks. *Phys. Rev. E*, **71**, 16–106.
- Doyle,J.C. *et al.* (2005) The ‘robust yet fragile’ nature of the internet. *Proc. Natl Acad. Sci. USA*, **102**, 14497–14502.
- Erdős,P. and Rényi,A. (1959) On random graphs. *Publ. Math.*, **6**, 290–297.
- Erdős,P. and Rényi,A. (1960) On the evolution of random graphs. *Publ. Math. Inst. Hung. Acad. Sci.*, **5**, 17–61.
- Giot,L. *et al.* (2003) A protein interaction map of *Drosophila melanogaster*. *Science*, **302**, 1727–1736.
- Han,J.D.H. *et al.* (2005) Effect of sampling on topology predictions of protein–protein interaction networks. *Nat. Biotechnol.*, **23**, 839–844.
- Ito,T. *et al.* (2000) Toward a protein–protein interaction map of the budding yeast: a comprehensive system to examine two-hybrid interactions in all possible combinations between the yeast proteins. *Proc. Natl Acad. Sci. USA*, **97**, 1143–1147.
- Jeong,H. *et al.* (2000) The large-scale organization of metabolic networks. *Nature*, **407**, 651–654.
- Jeong,H. *et al.* (2001) Lethality and centrality in protein networks. *Nature*, **411**, 41–42.
- Kashtan,N. *et al.* (2004) Efficient sampling algorithm for estimating subgraph concentrations and detecting network motifs. *Bioinformatics*, **20**, 1746–1758.
- Lappe,M. and Holm,L. (2004) Unraveling protein interaction networks with near-optimal efficiency. *Nat. Biotechnol.*, **22**, 98–103.
- Li,L. *et al.* (2005) Towards a theory of scale-free graphs: definition, properties, and implications (extended version). arXiv:cond-mat/0501169.
- Li,S. *et al.* (2004) A map of the interactome network of the metazoan *C. elegans*. *Science*, **303**, 540–543.
- Maslov,S. and Sneppen,K. (2002) Specificity and stability in topology of protein networks. *Science*, **296**, 910–913.
- Milo,R. *et al.* (2002) Network motifs: simple building blocks of complex networks. *Science*, **298**, 824–827.
- Milo,R. *et al.* (2004) Superfamilies of evolved and designed networks. *Science*, **303**, 1538–1542.
- Newman,M.E. and Watts,D.J. (1999a) Renormalization group analysis in the small-world network model. *Phys. Lett. A*, **263**, 341–346.
- Newman,M.E. and Watts,D.J. (1999b) Scaling and percolation in the small-world network model. *Phys. Rev. E*, **60**, 7332–7342.
- Penrose,M. (2003) *Geometric Random Graphs*. Oxford University Press, Oxford, UK.
- Peri,S. *et al.* (2004) Human protein reference database as a discovery resource for proteomics. *Nucleic Acids Res.*, **32**, D497–D501, 1362–4962, (Journal Article).
- Pržulj,N. *et al.* (2004) Modeling interactome: scale-free or geometric? *Bioinformatics*, **20**, 3508–3515.
- Pržulj,N. *et al.* (2006) Efficient estimation of graphlet frequency distributions in protein–protein interaction networks. *Bioinformatics*, **22**, 974–980.
- Rual,J.-F. *et al.* (2005) Towards a proteome-scale map of the human protein–protein interaction network. *Nature*, **437**, 1173–1178.
- Shen-Orr,S.S. *et al.* (2002) Network motifs in the transcriptional regulation network of *Escherichia coli*. *Nat. Genet.*, **31**, 64–68.
- Simon,H.A. (1955) On a class of skew distribution functions. *Biometrika*, **42**, 425–440.
- Stelzl,U. *et al.* (2005) A human protein–protein interaction network: a resource for annotating the proteome. *Cell*, **122**, 957–968.
- Stumpf,M.P.H. *et al.* (2005) Subnets of scale-free networks are not scale-free: Sampling properties of networks. *Proc. Natl Acad. Sci. USA*, **102**, 4221–4224.
- Tanaka,R. (2005) Scale-rich metabolic networks. *Phys. Rev. Lett.*, **94**, 168101.
- Uetz,P. *et al.* (2000) A comprehensive analysis of protein–protein interactions in *Saccharomyces cerevisiae*. *Nature*, **403**, 623–627.
- Vazquez,A. *et al.* (2004) The topological relationship between the large-scale attributes and local interaction patterns of complex networks. *Proc. Natl Acad. Sci. USA*, **101**, 17940–17945.
- von Mering,C. *et al.* (2002) Comparative assessment of large-scale data sets of protein–protein interactions. *Nature*, **417**, 399–403.
- Watts,D.J. and Strogatz,S.H. (1998) Collective dynamics of ‘small-world’ networks. *Nature*, **393**, 440–442.
- West,D.B. (2001) *Introduction to Graph Theory*, 2nd edn. Prentice Hall, Upper Saddle River, NJ.
- Yeger-Lotem,E. *et al.* (2004) Network motifs in integrated cellular networks of transcription-regulation and protein–protein interaction. *Proc. Natl Acad. Sci. USA*, **101**, 5934–5939.
- Zanzoni,A. *et al.* (2002) Mint: a molecular interaction database. *FEBS Lett.*, **513**, 135–140.